Effect of Triclosan on Self-Assembly of Alkyl Ammonium Surfactants Adsorbed within Montmorillonite Galleries in Silicone Elastomer Composites

Christopher M. Liauw,*[1] *Rebecca L. Taylor*,[2] *Lindsey J. Munro*,[3] *Arthur N. Wilkinson*,[3] *Onanong Cheerarot*[4]

Summary: Poly(propylene) homopolymer/fly ash (50% wt) composites have been prepared from two samples of fly ash that differ in terms of the geographic source of coal feedstock, which left one of the samples with a higher group I and II metal content. A screening study indicated that Lubrizol Solplus® C800 (an unsaturated carboxylic acid dimer coupling agent), initiated with dicumyl peroxide, conferred the best strength–toughness balance to the composites. In some cases, however this was related to detachment of the interfacial region due to possible extraction of PP-C800 adduct-group I and II ion reaction products. Interfacial adhesion was arguably too high in the case of the fly ash sample bearing a lower level of group I and II ions. These deductions were also supported by DSC data.

Keywords: composite; coupling agent; fly ash; β-poly(propylene); poly(propylene)

Introduction

Triclosan [5-chloro-2-(2,4-dichlorophenoxy)-phenol] (TCS) is an effective broad spectrum antimicrobial that has the potential to retard microbial colonisation of maxillofacial appliances based on polydimethylsiloxane (PDMS) elastomers. TCS is not soluble in PDMS and therefore will form separate domains in the elastomer and a surface bloom. This incompatibility leads to excessively fast release which would fail to increase longevity of the prosthesis as microbial attachment would resume.

In the last Eurofillers paper [1] on this subject we investigated the adsorption interaction (from heptane) between TCS and a variety of different o-MMTs using flow micro-calorimetry. We found that Rockwood / Southern Clay Products Cloisite 15A (C15A) interacted most prolifically with TCS and that this o-MMT gave the most sustained release of TCS from a PDMS based composite into water.[1] Whilst it was significant that C15A showed the greater affinity for TCS during adsorption from heptane, the amount adsorbed was not sufficient to fully explain the controlled release behaviour. Wide angle X-ray scattering revealed that C15A platelets in the composites showed increase uniformity of spacing relative to the other o-MMTs; some form of co-intercalation was proposed but not investigated.

The objective of this paper is to investigate the co-intercalation of MMT by dihydrogenatedtallow dimethyl ammonium and TCS and how such interactions affect the interlayer spacing and uniformity thereof. The study will make use of C15A and

[1] Centre for Materials Science Research, Manchester Metropolitan University, Chester Street, Manchester M1 5GD, UK
E-mail: c.m.liauw@mmu.ac.uk
[2] School of Healthcare Science, Manchester Metropolitan University, Chester Street, Manchester, M1 5GD, UK
[3] School of Science and the Environment, Manchester Metropolitan University, Chester Street, Manchester M1 5GD, UK
[4] School of Materials, The University of Manchester, Grosvenor Street M1 7HS, UK

Cloisite 20A (C20A), which are loaded with 136% and 100% CEC, respectively of the latter surfactant. The dispersion of the o-MMT platelets will be monitored using WAXS, composite mechanical response and TCS release behaviour. The heat of formation of the proposed co-intercalate structures will then be simulated using molecular modelling software. The role of unbound surfactant on the formation of the co-intercalate structures will also be investigated by removal of the unbound surfactant from C15A and C20A by Soxhlet extraction with heptane

Experimental Part

The formulations were based on addition cured (Hydrosilylation – Platinum catalysed) silicone elastomer (PDMS [Cosmesil Pricipality Medical Ltd.]). The o-MMTs used were Rockwood Additives/Southern Clay Products Cloisite® 15A (C15A) and Cloisite® 20A (C20A), both these o-MMTs are intercalated with dihydrogenated-tallow-dimethylammonium chloride, tallow is assumed to be composed of 65% C18, 30% C16 and 5% C14. Surfactant levels are shown in Table 1. Unmodified MMT (Rockwood/Southern Clay Products Cloisite Na+ (CNa+)) was used for the preparation of control samples. The o-MMT was blended with the silicone resin at 60 °C to ensure melting of the TCS crystals and optimal dispersion and adsorption in to the o-MMT.

The aim of the first study was to investigate the effect of TCS level on the state of dispersion of C15A platelets in PDMS whilst the level of C15A was held constant at 15% wt. TCS level ranged from 6.67 g to 40.00 g/100g C15A. Control formulations containing 3% wt TCS in PDMS and PDMS only were also prepared. Composite plaques were cast at room temperature using PMMA moulds.

The mechanical properties of the composites were measured at ambient temperature using BS903 A2 dumbbells, punched from the composite sheets. They were held in a Hounsfield H10 KS tensometer using self-tightening roller grips. Cross head speed was at 100 mm min^{-1} and strain was measured using a laser extensometer. Stress values were recorded at the following strains; 25, 50, 100, 200, 300%. Values of tensile strength and elongation at break were also recorded. At least seven replicates were tested from each composite and the average and standard deviation were determined using the closest five values. WAXS data was obtained using a Philip X'pert-MPD diffractometer fitted with a copper tube, the anode voltage and current were 45 kV and 40 mA, respectively and scan rate (from 1° to 25°) was 0.43° min^{-1} (Step size was 0.05° with a counting time of 7 s). The moulded surfaces of the composite coupons (supported on microscope slides) were exposed to the beam. The leaching study was carried out using squares (1 cm x 1 cm) of composite cut from the moulded sheets which were then weighed before being placed in a glass universal bottle containing deionised water (20 ml). The latter was then agitated at 37 °C in an orbital incubator. The water was changed every three days in order to minimise equilibration of leaching due to

Table 1.
Surfactant levels and asymmetric C-H stretching frequency ($\nu_{(-CH-H)as}$) for o-MMTs investigated.

o-MMT	Surfactant level (measured)			Surfactant level (data sheet)			$\nu_{(-CH-H)as}$ (cm^{-1})	$d_{(001)}$ (nm)
	% wt	mmol g^{-1}	% CEC	% wt	mmol g^{-1}	% CEC		
C15A	39.3	1.20	130	40.3	1.25	136	2919.7	2.9
Ext. C15A	35.0	1.00	109	–	–	–	2922.8	2.3
C20A	34.7	0.99	108	33.9	0.95	103	2922.3	2.5
Ext. C20A	33.1	0.91	99	–	–	–	2923.5	2.2

Ext. – Soxhlet extracted with propan-2-ol for 10 hours.

saturation of the solution with TCS. The concentration of TCS in the water was determined after 48, 336 and 840 hours leaching by UV spectroscopy (at $\lambda_{max} = 198$ nm $\pm$ 2 nm). After the leaching period (840 hours) the samples were immediately weighed and water sorption calculated.

The second study involved examining the effect of unbound surfactant and small variation of the added surfactant level on the state of dispersion of the o-MMT platelets and the concomitant effect on TCS release into water. The unbound surfactant was removed from the o-MMTs by 10 hour Soxhlet extraction with propan-2-ol, followed by removal of the propan-2-ol by evaporation at ambient temperature for 16 hours in the draft of a fume cupboard then 16 hours in an oven at 80 °C. The caked extracted o-MMT was then re-micronised using a Waring blender. Surfactant levels in the o-MMTs were determined from mass loss on ignition at 700 °C, after taking account of the lattice water. All o-MMTs were examined using diffuse reflectance Fourier transform infrared spectroscopy (DRIFTS) in order to acquire some insight into the relative ordering of the surfactant alkyl chains. DRIFTS was carried out using a Thermo-Nicolet Nexus fitted with a Spectra-Tech DRIFTS cell, spectra were made up of 164 scans with resolution set to 4 cm^{-1}.

The composite formulations are based on equivalent MMT silicate levels, i.e. the level of o-MMT/extracted o-MMT was varied so as to give a constant MMT silicate level. Following on from the previous study, the silicate level was based on that in a composite containing 15% wt C15A. The TCS to MMT silicate ratio was kept constant at 49.45 g/100g MMT silicate (equivalent to 30 g / 100g C15A). Control formulations containing 9.1% wt Cloisite Na+ with 4.5% wt TCS, 4.5% wt TCS in PDMS and PDMS only were also prepared. Composite plaques were cast at room temperature using PMMA moulds as previously described and the plaques were subjected to the same analyses as for the first study.

The third study involved using computational modelling to probe the thermodynamic stability of three distinct models: (i) distearyldimethylammonium $(CH_3)_2(C_{18}H_{37})_2N^+$, (ii) a bimolecular pore made up of two distearyldimethylammonium surfactant molecules and (iii) the bimolecular surfactant pore with two molecules of TCS interacting with the surfactant molecules. The optimum geometry for each model was determined using a combination of conformational searching and optimisation with a semi-empirical level of theory, PM3. [2–3].

Results and Discussion

The surfactant levels in the o-MMTs before and after extraction are shown in Table 1. It is evident that C15A has a high surfactant dosage that is beyond the CEC of the MMT; the experimentally determined surfactant dosage agrees closely with the manufacturer's figures. Extraction of C15A with propan-2-ol reduced the surfactant level to just slightly above 100% CEC. C20A has a surfactant level in the unextracted state that is very close to that of extracted C15A, again the measured surfactant level for C20A is close to that quoted by the manufacturer. Extraction of C20A results in a further reduction in surfactant level down to sensibly 100% of CEC. Asymmetric methylene stretching vibration frequencies ($\nu_{(-CH-H)as}$) for the o-MMTs obtained from DRIFTS Spectra are also shown in Table 1; as the level of surfactant decreases, $\nu_{(-CH-H)as}$ generally increases due to the chains being in an increasingly liquid-like state [4–5]. This demonstrates that as surfactant level reduces chains become less well packed thereby indicating that the unbound surfactant resides in gaps between molecules of bound surfactant. It should be pointed out that alkyl chains packed in to a crystalline (all trans conformation) array have $\nu_{(-CH-H)as}$ closer to 2818 cm^{-1} that is accompanied by splitting of the methylene rocking bands (735–715 cm^{-1}) [6–7]. These conditions were not met in any of the samples and hence indicated that

packing of the alkyl chains was not as ordered as it could be, perhaps due to the mixture of alkyl chain lengths.

A plot of concentration of TCS in the leaching liquor at 410 hours leaching versus the level of TCS relative to o-MMT is shown in Figure 1. TCS addition levels of 6.67 to 13.33 g/100g C15A effectively show zero leaching, however, increasing the TCS level beyond 13.33 g/100g results in TCS being observed in the leaching liquor and TCS levels greater than the latter result in a linear increase in the amount leached out. A data point corresponding to the equivalent TCS level in the formulation containing 3%wt TCS with no C15A is also included in Figure 1 and dramatically illustrates the controlled release behaviour imparted by TCS interactions with C15A. The level of TCS adsorbed by C15A from heptane (FMC study [1]) was 12 g /100g a figure that corresponds well with the threshold TCS level for leaching.

Composite stiffness is a measure of interfacial area in the composite and therefore a measure of the extent of dispersion of agglomerates into tactoids, and perhaps to a lesser extent separation of tactoids into individual platelets. Figure 2 shows the stress at 20% strain (M_{20}) and 50% strain (M_{50}) as a function of TCS level.

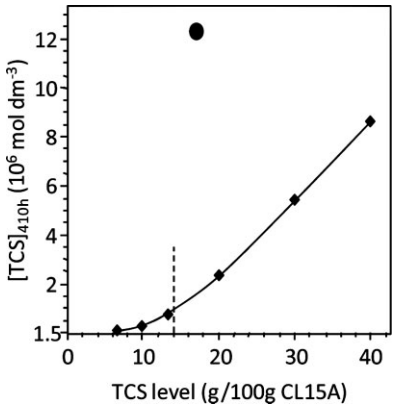

Figure 1.
Concentration of TCS leached from the composites after 410 hours in water at 37 °C, versus TCS level. The single oval data point represents the leached concentration for a composite containing no C15A.

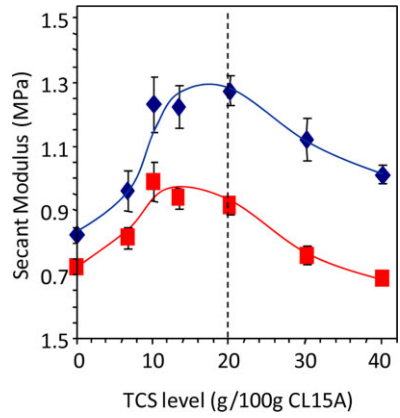

Figure 2.
Secant modulus between; ◆, 0 and 20 % strain (M_{20}) and ■, 0 and 50 % strain (M_{50}), versus TCS level.

It is evident that stiffness reached a maximum at a TCS level which roughly corresponds to that where TCS is observed in solution (Figure 1) and that determined by FMC adsorption from heptane. Therefore it is highly likely that a critical amount of TCS is required to allow the PDMS chains to intercalate the tactoids and split them up. As the TCS level corresponded to the FMC determined level it is likely that the adsorption sites concerned are the hydroxyl groups at the platelet edges. Blockage of these sites has been shown by other researchers [8] to facilitate intercalation of the galleries by polymer chains because they are no longer able to get stuck to the platelet edges and block entry of chains into the gallery. Further increases in the TCS level caused a reduction in stiffness which maybe explained by a decrease in interfacial adhesion and/or re-aggregation of the platelets and/or plasticization of the matrix by TCS. The first explanation unlikely because the dehydrogenated tallow dimethyl ammonium that covers the basal surfaces will already provide low levels of interfacial adhesion without co-adsorbed TCS. As the TCS forms a separate phase in the matrix (see WAXS and DSC data later) it is unlikely that matrix plasticization occurs to a significant extent. Therefore re-aggregation is the favoured

explanation, an effect that was confirmed by WAXS and further corroborated by the increasing difference between M_{20} and M_{50} observed at TCS levels beyond 10 g TCS / 100 g C15A.

Breakdown of tactoids at higher strains will dramatically reduce their stiffening effect and hence reduce M_{50}.

The family of WAXS data showing the effect of TCS level on the distribution of C15A platelets is shown in Figure 3. It is evident that low levels of TCS led to (001) reflections of significantly reduced intensity and that (001) intensity reaches a minimum at 20 g TCS / 100 g C15A. Further addition of TCS leads to an increase in both (001) intensity and the appearance of higher order reflections combined with a significant narrowing of the reflection peaks. The normalised (001) intensity is plotted against the level of TCS added in Figure 4, where the minimum can be clearly observed to coincide precisely with the maximum in stiffness and is close to the level of TCS adsorbed as measured by FMC. This observation supports the idea that tactoids have substantially split up, giving an increase in interfacial area which explains the increase in stiffness. The increase in (001) intensity combined with peak narrowing and higher order reflections indicates that the reduction in stiffness is not due to simple random re-aggregation of the platelets but rather due to controlled re-stacking [9] which appears to be triggered by adsorption of a critical level of TCS.

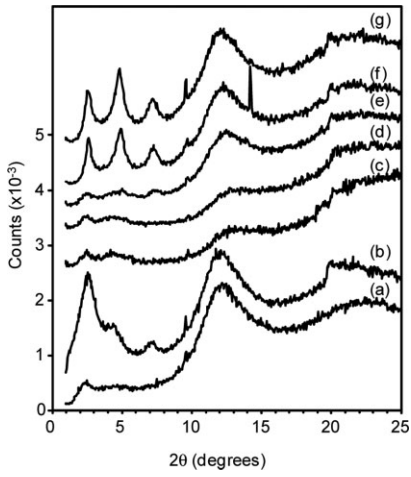

Figure 3.
WAXS data for (a) unfilled matrix and samples containing C15A with increasing levels of TCS (g TCS / 100 g C15A); (b) 6.67, (c) 10.00, (d) 13.33, (e) 20.00, (f) 30.00 and (g) 40.00.

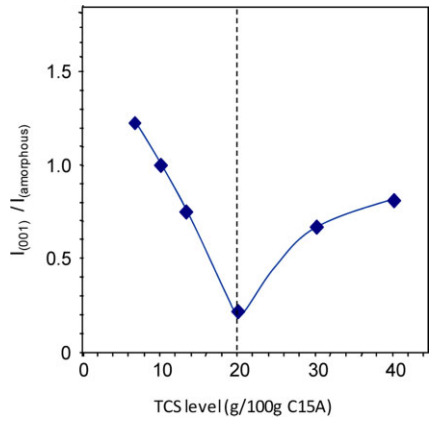

Figure 4.
Ratio of (001) reflection intensity ($I_{(001)}$) to the intensity of the amorphous halo ($I_{(amorphous)}$), versus TCS level.

The broad (001) reflection observed at 6.67 g TCS / 100 g C15A suggests that whilst the average interlayer spacing is 2.4 nm, there is a considerable degree of stacking disorder [9]. Increasing levels of TCS result in blockage of the platelet edge hydroxyl groups which facilitates intercalation of PDMS and eventual splitting up of the tactoids. The interlayer spacing of 2.4 nm is retained, even at higher TCS levels (where increased ordering was observed) and is consistent with that for a slanted C18 alkyl chain. Pukánszky's group have examined the arrangement of surfactant alkyl chains in MMT galleries and for dialkyl types they propose that one of the C18 chains points away from the basal surface in a slanted manner and the other chain lies along the basal surface [10]. A surfactant molecule adsorbed in this manner can then interact with others as shown in Figure 5, forming self-assembled pore-like structures. In C15A it is clear that the alkyl tails are not adsorbed in such a uniform manner

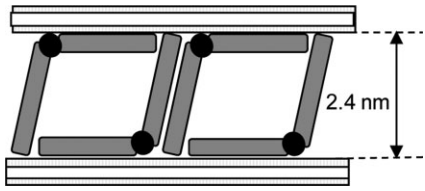

Figure 5.
Schematic representation of alkyl chain arrangement in distearyl ammonium surfactants as proposed by Pukánszky et al. [10].

when TCS is absent, however addition of TCS causes the chains to "snap" into the arrangement proposed by the Pukánszky group. This aspect was discussed in the previous Eurofillers paper though the WAXS data obtained at that time was not so convincing.

The heat of formation of the arrangement proposed by the Pukánszky group (considering just two molecules of surfactant) has been determined from the optimised energies of the monomolecular and bimolecular surfactant models; a value of $+27.2\,kJ\,mol^{-1}$ was obtained indicating an endothermic process, when starting from single molecules. In contrast, the heat of formation of the optimised co-intercalated structure in which TCS interacts with the aminyl nitrogen of the surfactant is exothermic ($-42.0\,kJ\,mol^{-1}$). Whilst the model ignores interactions with neighbouring surfactant molecules (which is likely to cause the heat of formation of the homo-intercalate to become exothermic), the change from endothermic to exothermic resulting from adsorption of TCS is significant and supports the co-intercalation hypothesis mooted in the previous paper. Due to consideration of only two surfactant molecules in the simulation, the slanted arrangement proposed by Pukánszky has not been predicted.

In order to form such self-assembled structures there must arguably be a critical level of surfactant present and a significant fraction of it must be mobile and not strongly bound to the regions of negative charge originating from the mixed oxide based mid-layer of the platelets. This idea was tested by using an o-MMT with a reduced level of surfactant (i.e. C20A) and C15A and C20A which have been extracted with propan-2-ol in order to remove the unbound surfactant. The effect on WAXS data is shown in Figures 7 and 8 for composites based on C20A and C15A, respectively. WAXS data for TCS is also included to show the positions of reflections from this highly crystalline solid. DSC

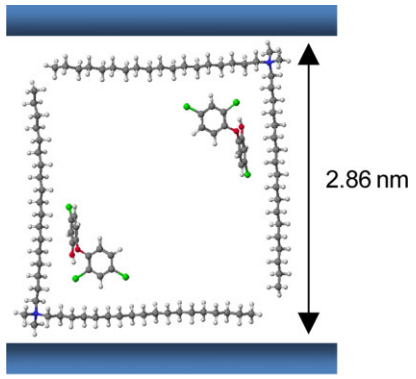

Figure 6.
Illustration of the bi-molecular surfactant model of the co-intercalate, resulting from simulation. The heat of formation of this arrangement is exothermic even though only two surfactant molecules are considered in the simulation.

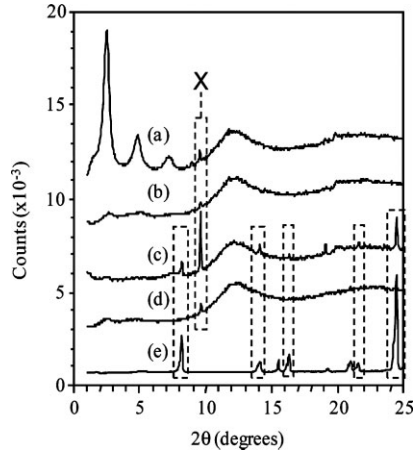

Figure 7.
WAXS data for PDMS/o-MMT/TCS composites; (a) unextracted C15A – TCS, (b) extracted C15A – TCS, (c) Na-MMT – TCS, (d) Unfilled TCS, (e) TCS only (reduced to fit). The reflection marked X is unidentified.

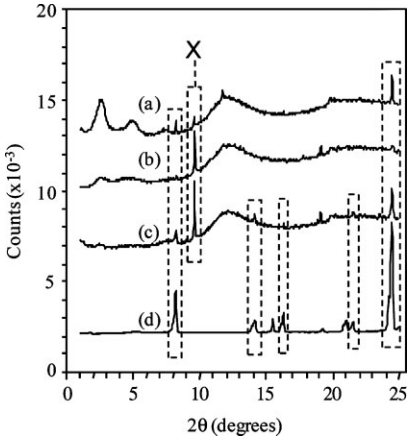

Figure 8.
WAXS data for PDMS/o-MMT/TCS composites; (a) unextracted C20A – TCS, (b) extracted C20A – TCS, (c) Na-MMT – TCS, (d) TCS only (reduced to fit). The reflection marked X is unidentified.

(Figure 9) was also carried out on these composites in order to observe melting of TCS domains. Reducing the level of surfactant initially added (without removing the unbound content) has minimal effect on the ability to form the self assembled surfactant structures, though

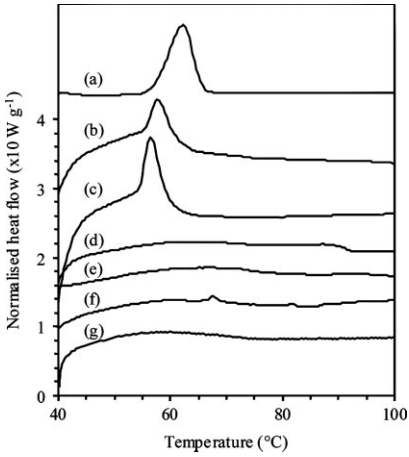

Figure 9.
DSC data for (a) TCS powder, (b) PDMS / TCS, (c) PDMS / Na + MMT / TCS, (d) and (e) PDMS / C15A / TCS (unextracted and extracted, respectively, (f) and (g) PDMS / C20A / TCS (unextracted and extracted, respectively). Note, sample masses are normalised to the mass of TCS in the sample.

the overall intensity of the reflections is somewhat lower than for the equivalent C15A based composite. This observation implies that not all of the platelets were arranged into uniform stacks. The latter is supported by the appearance of some weak reflections assignable to crystalline domains of TCS, evidence for the latter may be supported by a very small melting endotherm peak for TCS in the DSC data. The presence of crystalline TCS demonstrates that there was insufficient surfactant to bind all the TCS present. Extraction of unbound surfactant from both C15A and C20A results in an inability to form the ordered platelet stacks previously observed. It is highly likely that this stems from it being no longer possible to form the self-assembled surfactant structures due to there being no unbound surfactant to move into gaps between the strongly adsorbed surfactant molecules.

Whilst the ability to form self-assembled surfactant structures has been lost as a result of removal of unbound surfactant, it is apparent from the WAXS and DSC data that there is no sign of crystalline domains of TCS. Loss of the TCS melting endotherm in the case of the extracted C20A based composite indicates possible adsorption of TCS onto basal surfaces. This indicates that the interactions between surfactant and TCS are still intact.

Examination of the release characteristics into water (Figure 10) shows that the reduced surfactant level in C20A led to an initially faster rate of release which then reduced to a level similar to that afforded by C15A. The relatively high initial rate of release observed with C20A may therefore be related to the TCS that is not coordinated with surfactant molecules. Extraction of unbound surfactant from both C20A and C15A resulted in an increase in the leached concentration with both extracted o-MMTs promoting almost exactly the same release characteristics. Considering the similarity in the surfactant levels after extraction (Table 1) this observation was not unexpected and may also support the proposed adsorption of TCS on basal surfaces between strongly bound surfactant molecules.

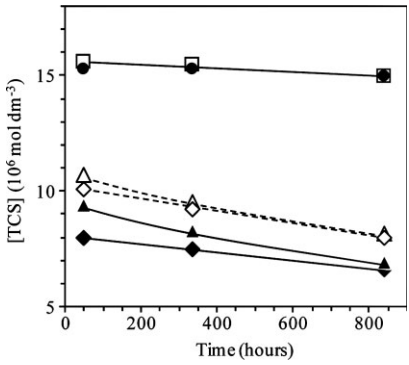

Figure 10.
Leaching data for: ◆ C15A TCS, Δ▲ C20A – TCS (solid symbols unextracted o-MMT, open symbols extracted o-MMT). □ Na+MMT – TCS, ● TCS only.

The TCS release characteristics for the TCS/NaMMT/PDMS and TCS/PDMS are also shown on Figure 10; whilst extraction of unbound surfactant from C15A and C20A increased the leached concentration relative to the unextracted o-MMTs, it is evident that the level of increase was rather insignificant considering the loss of the uniformly spaced platelets observed in composites based on the unextracted o-MMTs. Water sorption data is shown in Figure 11. Predictably very little water was absorbed by the unfilled PDMS and the loss of TCS dominated any water pick-up in the PDMS / TCS control. Due to the organophillic (hydrophobic) nature of the o-MMT galleries, composites based on both unextracted C15A and C20A (both with TCS) had much reduced water pick-up than that based on CNa+ / TCS. Due to the presence of the Na+ ions, the latter has a hydrophilic gallery. Extraction of the unbound surfactant led to similar increases in water pick-up in both C20A and C15A based composites. For the o-MMT based composites, water sorption characteristics mirrored the TCS release behaviour; low water sorption went hand in hand with low leached concentrations of TCS.

In the case of composites based on extracted o-MMT, water may displace TCS from adsorption sites that would otherwise have been occupied by unbound surfactant. In the previous paper we proposed that the moderated release was due to the adsorption of TCS within pores made up from the self-assembled surfactant alkyl chains. The observations made during the current study show that this is not the case. The interaction between the surfactant aminyl nitrogen and TCS is the dominating factor and self-assembly of surfactant alkyl chains into the proposed rhomboid section pore structures played a relatively minor role in moderating the release TCS.

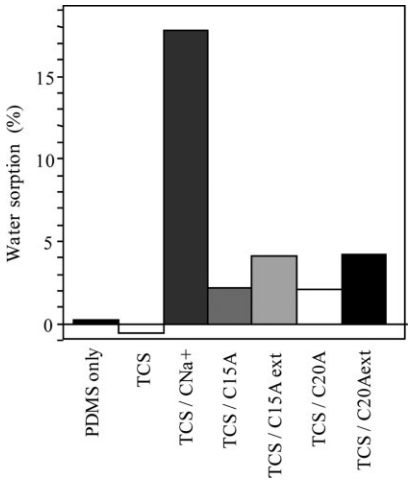

Figure 11.
Water sorption data for PDMS / o-MMT / TCS composites.

Conclusion

Interaction of TCS with dihydrogenated-tallowdimethylammonium adsorbed within the galleries of C20A and C15A in a PDMS matrix facilitates self-assembly of the hydrogenated tallow chains, provided there is sufficient TCS added to the formulation to allow interaction of one TCS molecule with one surfactant molecule. This effect led to re-aggregation of the o-MMT platelets into highly ordered stacks that gave rise to narrow and intense reflection peaks and higher order reflections. From the interlayer spacing of these highly ordered tactoids, we proposed that the tallow alkyl chains were arranged in a manner proposed by the Pukanszky group.

Computational calculations of optimised geometries using a bi-molecular model indicated an endothermic heat of formation for this arrangement whilst the heat of interaction between a TCS molecule and the aminyl nitrogen, together with steric effects, shifted the heat of formation of the structure from endothermic to exothermic. The self-assembled structure of hydrogenated tallow alkyl tails was considered to form pore like structures in which the TCS molecules resided. The interaction between TCS and the surfactant was strong enough to prevent TCS from forming a separate crystalline phase. Removal of unbound surfactant from the o-MMTs prior to addition to TCS/PDMS all but eliminated the ability to form the self-assembled surfactant structures and hence the highly ordered tactoids were not formed. The TCS, however, was nevertheless still prevented from forming a separate crystalline phase, indicating that the interactions between the aminyl nitrogen and TCS were still intact.

Leaching studies revealed that the above pore-like structures made from the self-assembled surfactant alkyl tails played a relatively minor role in terms of moderating the rate of release of TCS into water. The interaction between the aminyl nitrogen of the surfactant and TCS was by far the major factor influencing moderation of TCS release from the composites in to water.

Acknowledgements: Natasha Nadine William, Emma Williams and Peter Skingle of MMU for preparation and examination of the composites.

[1] C. M. Liauw, R. L. Taylor, C. Maryan, R. Kato, A. N. Wilkinson, O. Cheerarot, *Macromol. Symposia*, **2011**, *301*, 96.
[2] J. J. P. Stewart, *J. Comput. Chem.*, **1989**, *10*, 209.
[3] J. J. P. Stewart, *J. Comput. Chem.*, **1989**, *10*, 221.
[4] R. A. Vaia, R. K. Teukolsky, E. P. Giannelis, *Chem. Mater.* **1994**, *6*, 1017.
[5] C. M. Liauw, G. C. Lees, R. N. Rothon, A. N. Wilkinson, P. Limpanapittayatorn, *Composite Interfaces*, **2007**, *14*, 361.
[6] Y. Li, H. Ishida, *Langmuir* **2003**, *19*, 2479.
[7] R. G. Snyder, *J. Phys. Chem.* **1979**, *71*, 3229.
[8] J. G. Zhang, R. K. Gupta, C. A. Willkie, *Polymer*, **2006**, *47*, 4537.
[9] R. A. Vaia, W. Lui, *J. Polym. Sci. B. Polym. Phys.*, **2002**, *40*, 1590.
[10] F. Kádár, L. Százdi, E. Fekete, B. Pukánszky, *Langmuir*, **2006**, *22*, 7848.

